Journal of Nuclear Materials 518 (2019) 409–418

Contents lists available at ScienceDirect

Journal of Nuclear Materials

journal homepage: www.elsevier.com/locate/jnucmat

# Application of the small punch test in combination with the master curve approach for the characterisation of the ductile to brittle transition region

David Andres [a, b, *], Roberto Lacalle [b], Sergio Cicero [b], Jose A. Alvarez [b]

[a] Technology Department, UK Atomic Energy Authority, Culham Science Centre, Abingdon, Oxfordshire, United Kingdom
[b] LADICIM (Laboratory of Materials, Science and Engineering), University of Cantabria, Santander, Cantabria, Spain

## HIGHLIGHTS

- Small punch notched specimens can be applied to estimate the reference temperature.
- A methodology to estimate the reference temperature has been proposed.
- A single correlation has been obtained for the ferritic steels analysed.

## ARTICLE INFO

*Article history:*
Received 25 September 2018
Received in revised form
6 February 2019
Accepted 9 March 2019
Available online 13 March 2019

*Keywords:*
Small punch
Ductile to brittle transition region
Ferritic steels
Master curve
Reference temperature
Fracture

## ABSTRACT

The Master Curve approach allows the full characterisation of the ductile to brittle transition region (DBTR) of ferritic steels to be performed with a reduced number of tests. In this paper, the approach has been combined with the application of the small punch (SP) test. Modified SP specimens have been successfully employed to estimate the fracture toughness values of a pressure vessel steel and three structural steels. In addition, a methodology has been proposed, including a validity criterion for the performed tests. The estimated reference temperatures have been compared to the values obtained by means of full-scale conventional techniques. A unique simple relationship between both methodologies has been established for all the analysed materials. Therefore, this paper confirms the suitability of the small punch testing technique for the characterisation of the DBTR of several ferritic steels. It is a promising, simple and cost-effective test, which can be performed with simple equipment.



## 1. Introduction

Damage-tolerant designs or structural integrity assessments require the characterisation of damaged material under working conditions to evaluate the ageing of components during their service life. In the nuclear industry, materials are exposed to irradiation, which can lead to embrittlement, among other effects. In order to guarantee the operation of nuclear components under safe conditions and perform their assessment, an accurate characterisation of these effects is critical.

One of the main parameters to assess the influence of the irradiation embrittlement on ferritic steels is the reference temperature, $T_0$, employed in the Master Curve (MC) approach [1–4]. It enables the characterisation of the ductile to brittle transition region (DBTR) with a reduced number of tests, thanks to a combination of mechanistic modelling and a statistical approach. Moreover, it addresses the dependence on the thickness of the test sample and the scatter of the results in the DBTR. As a result, this parameter has been incorporated in several standards and codes, such as FKM-Guideline [1], BS 7910 [2], API 579/ASME FFS [3] or ASTM E1921 [4], among others.

The determination of $T_0$ has usually been performed by means of conventional fracture toughness tests. These require relatively large volumes of material, which is often not feasible for challenging nuclear applications, e.g. for the extension of the operation period of nuclear plants, since the material in the surveillance capsules is becoming scarce [5]. However, the MC approach allows specimens

* Corresponding author. Technology Department, UK Atomic Energy Authority, Culham Science Centre, Abingdon, Oxfordshire, United Kingdom.
*E-mail address:* david.andres@ukaea.uk (D. Andres).

https://doi.org/10.1016/j.jnucmat.2019.03.011
0022-3115/

of reduced thickness to be used [1–4]. As a result, large efforts are being done to develop small-scale testing techniques in combination with the MC, in order to further optimise the material [6]. For instance, micro-compact tension specimens of 10 × 10 × 4 mm have been successfully applied [7].

Currently, the small punch testing technique is one of the most promising miniature testing techniques. Evidence of this are the current efforts to establish a European standard to cover this methodology [8]. One of its most interesting applications is the estimation of fracture toughness by means of notched specimens of only 10 × 10 × 0.5 mm [9,10], something which is not possible to achieve by means of other miniature testing techniques for such reduced volumes of material.

In this paper, the use of the Master Curve approach in combination with small punch notched specimens is proposed to estimate the reference temperature on a wide range of materials: a pressure vessel steel (HSST plate 13B/A533B plate) and three structural steels (S275JR, S460M and S690Q). A relationship between the reference temperature obtained by means of small punch tests and by means of conventional testing techniques has been established. As a result, a methodology to estimate the reference temperature from small punch tests has been proposed.

## 2. Experimental device and materials

### 2.1. Experimental device and specimens

The small punch technique is a simple, cost-effective small sample test technique. It is a relatively recent test [11] that consists of punching a plate of only 0.5 mm-thickness with a 2.5 mm-radius punch passing through a 4 mm-diameter hole until rupture. Given the applicability of the technique and its potential there exists a European Code of Practice CWA 15627:2008 [12] and the technique is currently under standardisation process [8].

The testing procedure for the small punch tests followed in this paper is performed according to the recommendations of CWA 15627 [12]. The deformation of the test-piece has been monitored by means of the displacement of the punch tip, which is the distance by which the punch tip has moved after initial contact with the specimen surface. Since this movement cannot be measured directly, it has been estimated from the recorded crosshead displacement by subtracting the displacement corresponding to the push rod and the punch compliance to the crosshead displacement values. In order to be able to perform this operation, the compliance of the push rod and the punch was determined experimentally by punching a block of hard material instead of a small punch specimen, obtaining a value of ~$3*10^{-4}$ mm/N at room temperature. In addition, since the tests have been performed at various temperatures different from room temperature, the compliance has been corrected to consider this effect by applying the influence of temperature on the elastic modulus of steels proposed by BS 7910:2013 [2].

Since the goal of this paper is the estimation of the reference temperature (or the characterisation of the ductile to brittle transition region), the tests have been performed at low temperatures. To achieve these conditions, the testing rig has been assembled inside an environmental chamber. The chamber, shown in Fig. 1 and produced by DYCOMETAL, guarantees a stable temperature (±2 K) by regulating the liquid nitrogen input with a solenoid valve and a PID controller. In addition, a holding time of 10 min was applied once the target temperature was reached and before starting the test, to guarantee a homogenous temperature on the specimen. A universal machine with a load capacity of 2.5 kN has been employed, applying a crosshead displacement rate of 0.5 mm/min during the tests.

Regarding the specimens, the recommended geometry is 8 mm-diameter discs with 0.5 mm thickness [12]. In this paper, 10 × 10 mm square specimens of 0.5 mm-thickness have been employed. The use of this geometry eases the orientation of the specimens and enables the direct reutilisation of already tested Charpy specimens. Since the process area of the specimen under the punch remains constant and the clamped area is simply increased, it has already


**Fig. 1.** Environmental chamber and testing rig employed for the performance of the small punch tests.

been proved that the use of this geometry does not influence the obtained results [12–14]. To further guarantee the lack of influence of this change of geometry, simulations have been performed on both geometries, as shown in Appendix A, with matching results. As a result, the use of 10 × 10 mm specimens will be also included in the future European standard covering the small punch test on metallic materials.

To estimate fracture toughness, a modification of the specimens has been introduced. A lateral notch of 4.4 mm and 0.15 mm-radius has been machined, as shown in Fig. 2(C). The length of the notch has been chosen according to previous experience on materials with similar mechanical behaviours to guarantee the initiation of a crack during the test [5,9,10].

Several approaches have been employed to estimate fracture toughness to date. Some authors have correlated the equivalent fracture strain of ruptured unmodified small punch specimens with fracture toughness [15] or have established methods based on finite element simulations [16]. Other approaches are based on analytical solutions, which require the introduction of a defect on the specimen to initiate a crack; several geometries have been proposed to introduce such defect, such as the use of central notches [17], blind longitudinal notches [18] or circular notches [19], among others, as shown in Fig. 2 (A, B, D). The use of a lateral notch, chosen for this research, enables the orientation of the crack to analyse the direction of the material desired and its geometry can be easily machined by means of electrical discharge machining [9,10]. In addition, it has shown a good correlation with conventional full scale tests [9,10].

The specimens have been prepared according to the recommendations of CWA 15627 [12]. Firstly, the notch has been machined on 10 × 10 mm-section prisms. After this first step, the resulting pieces have been cut to 0.55 mm-thick pieces by means of a liquid-cooled cut-off machine and then ground to at least 2000 grit on both sides, until achieving the desired thickness of 0.5 ± 0.005 mm.

In addition, to avoid any possible influence of the notch geometry on the results, a special lower die has been used in the testing rig. During the tests, there can be some clearance between the specimen and the side walls of the lower die, especially when the dies have a circular shape and the specimens have a square shape. When small punch specimens without a notch are to be tested, this clearance does not introduce any changes to the results, since the clamped area around the punch axis remains greater than 8 mm-diameter. However, with the introduction of the lateral notch, it can lead to misalignments of the notch which result in modifications of the notch length, for instance. Consequently, an adjustable lower die with a rectangular shape has been designed, manufactured and utilised for testing this kind of specimens, which enables the reduction of the clearance to a minimum (Fig. 3). It is a novel design that enables the adjustment of the upper part of the lower die to each specimen individually. Furthermore, the use of this adjustable lower die makes it easier to correct any possible deviations from the desired notch length on the specimen, by simply grinding one of the edges until achieving the desired geometry, something that it is not possible to achieve with other testing rigs.

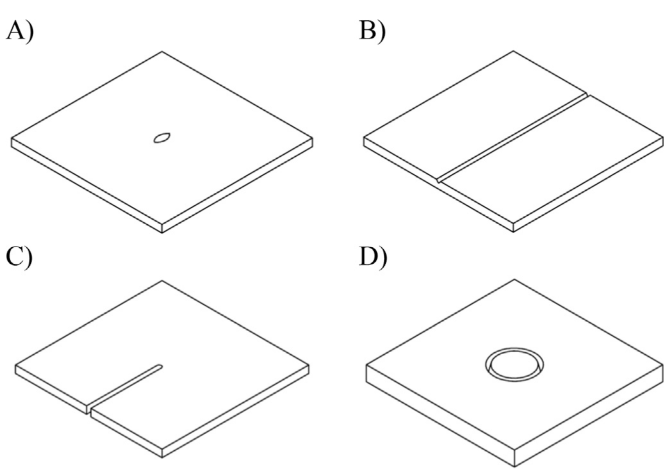


**Fig. 2.** Small punch specimens modified with a notch to estimate fracture toughness [20]: A) central notch [17], B) blind longitudinal notch [18], C) lateral notch [9,10], d) circular notch [19].

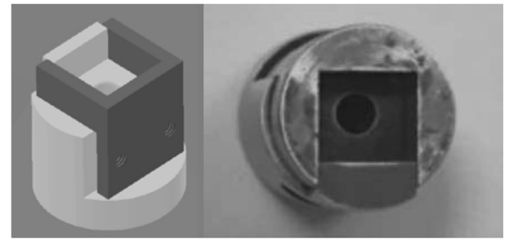

**Fig. 3.** Adjustable lower die [22].

The general alignment of the testing fixtures has been guaranteed by a manufacture process with a tolerance H7/h6, according to ISO 286-1 [21].

### 2.2. Materials

A pressure vessel steel (A533B 13B/A533B plate) and three structural steels (S275JR, S460M and S690Q) have been analysed in this research, covering a wide range of reference temperatures: from 160 to 250 K. Their chemical composition is shown in Table 1 and their mechanical properties are shown in Table 2. The reference temperature values have been obtained from (full-scale) 15 mm-thick SENB specimens for S460M and S690Q [23], 10 × 10 × 55 mm pre-cracked Charpy specimens for A533B [24] and 25 mm-thick CT specimens for S275JR [25].

## 3. Estimation of fracture toughness by means of notched small punch specimens

The estimation of fracture toughness by means of notched small punch specimens is based on the Crack Tip Opening Displacement (CTOD) approach [9,10]. The CTOD approach, and in the same way

**Table 1**
Chemical composition of the steels analysed (% weight) [23–25].

| | A533B | S275JR | S460M | S690Q |
|---|---|---|---|---|
| C | 0.12 | 0.18 | 0.18 | 0.15 |
| Si | 0.45 | 0.26 | 0.24 | 0.40 |
| Mn | 1.49 | 1.18 | 1.41 | 1.42 |
| P | 0.012 | 0.012 | 0.009 | 0.005 |
| S | 0.001 | <0.009 | 0.005 | 0.001 |
| Ni | 0.016 | <0.085 | 0.56 | 0.16 |
| Cr | 0.062 | <0.018 | 0.18 | 0.02 |
| Mo | 0.001 | <0.12 | 0.49 | 0.002 |
| V | 0.066 | <0.020 | 0.005 | 0.058 |
| Cu | 0.011 | <0.06 | 0.01 | 0.01 |
| Ti | 0.03 | <0.022 | – | 0.003 |
| Al | 0.048 | 0.034 | 0.021 | 0.056 |
| Fe | BAL. | BAL. | BAL. | BAL. |

**Table 2**
Mechanical properties of the analysed materials [23–25].

| | A533B | S275JR | S460M | S690Q |
|---|---|---|---|---|
| $\sigma_y$ [MPa] | 480 | 328 | 484 | 776 |
| $\sigma_u$ [MPa] | 608 | 519 | 594 | 834 |
| $T_0$ [K] | 250 | 247 | 181 | 162 |

the $J$ contour integral, can be used as a fracture criterion under elastic-plastic fracture mechanics (EPFM) conditions, i.e. to materials that exhibit time-independent nonlinear behaviour [26]. According to this approach, under EPFM conditions, a crack experiences a certain degree of blunting before fracture. The opening at the crack tip (*CTOD*) at the moment of the crack initiation, $\delta$, has been proved to be dependent on the material and can be directly used as a measure of fracture toughness [26]. Consequently, it can be directly correlated with the material critical $J$ contour integral. Shih [27] established a relationship between both parameters by evaluating the displacements at the crack tip implied by the HRR solution [24], as shown in eq. (1). It incorporates a dimensionless constant, $d_n$, that has a strong dependence on the strain hardening exponent of the material [27].

$$\delta = \frac{d_n J}{s_y} \tag{1}$$

where $s_y$ represents the yield stress of the material.

When a small punch test is being performed on a specimen with a lateral notch (Fig. 2(C)), the notch experiences a deformation similar to notch blunting, as shown in Fig. 4. At a certain point, usually at maximum force, a crack initiates from the notch tip. On the Force-Displacement curve obtained during the test, this crack initiation can be identified as an abrupt change on its slope, as shown in Fig. 5 [9,10].

By applying finite element simulations, a geometrical relationship between the punch displacement and the degree of blunting of the notch ($\delta_{SP}$) for a given notch length can be obtained [9,10]. In this paper, an elasto-plastic continuum mechanics finite element model realised via ANSYS version 18.0 was used to simulate a punch head going into a 10 × 10 mm sample with 4.4 mm-length notch with notch diameter of 0.30 mm. Only half of the specimen has been modelled, as shown in Fig. 4, given the symmetry of the specimen. The elements Tet10, Hex20 and Wed15 have been employed. The applied material properties have been derived from conventional testing, by using the elastic modulus of the material and a Ramberg-Osgood model for the hardening of the material. Frictional contacts have been employed, with a friction coefficient of 0.21. The load has been applied as a vertical displacement of the punch.

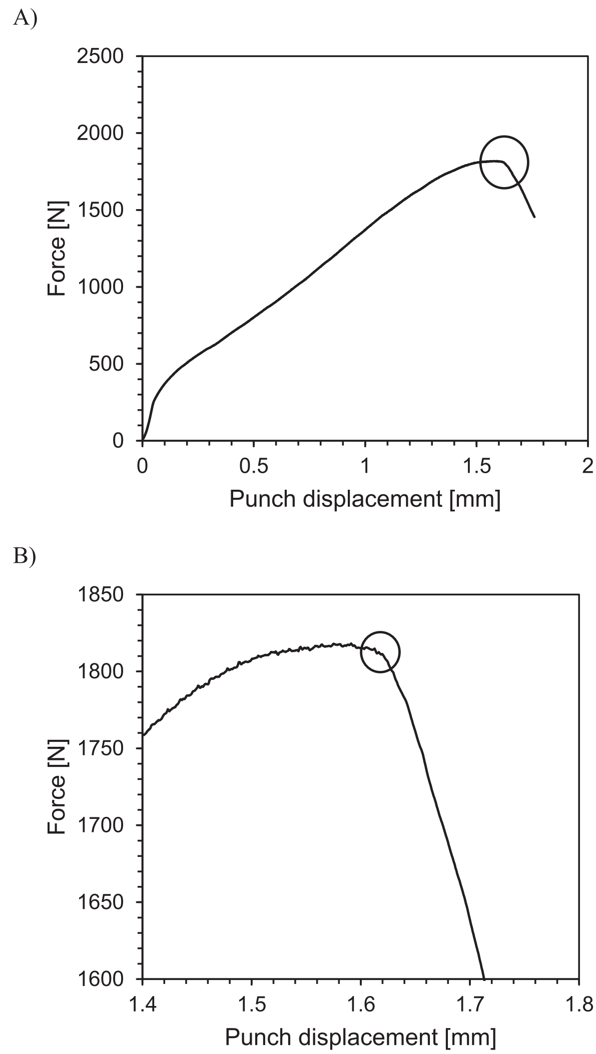


**Fig. 5.** Force-displacement curve of small punch test on a notched specimen, on which the crack initiation has been identified: A) whole curve, B) detail of the abrupt change of the slope.

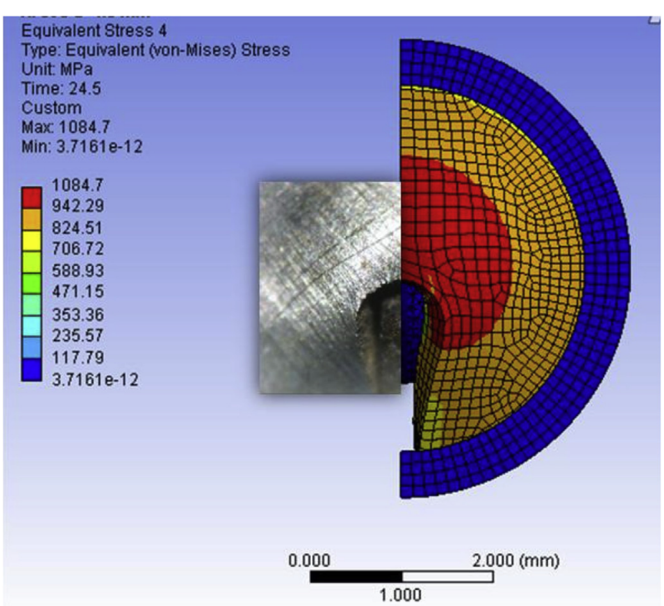


**Fig. 4.** Image of an interrupted test and the corresponding finite element simulation showing the deformation experienced by the notch during the test [14]. A 8 mm-diameter specimen has been used in this case to reduce the number of nodes, since according to section 2.1 it does not exhibit any influence on the results obtained.

The simulation provided the curve shown in Fig. 6, taking $\delta_{SP}$ as the average of the maximum opening of the notch at the upper and lower surface of the specimen. Furthermore, since the relationship between $\delta_{SP}$ and the punch displacement shown in Fig. 6 is material independent [9], the same estimated curve can be applied on all materials.

As a result, for each particular notch length, once the punch

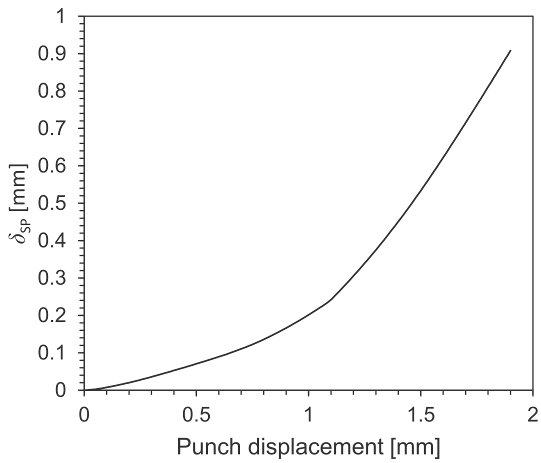


**Fig. 6.** Δsp-punch displacement curve obtained for a 4.4 mm-length notch by means of finite element simulations.

displacement at crack initiation has been obtained during the small punch test, the corresponding $\delta_{SP}$ can be identified by simply applying the corresponding $\delta_{SP}$ − Punch displacement curve, as that shown in Fig. 6. By appling eq. (1), this $\delta_{SP}$ value can be easily transformed into a SP measurement of the J-integral, $J_{SP}$, if the tensile properties of the material have already been obtained, something which can also be achieved by means of small punch tests. However, in this paper, the tensile properties of the materials analysed have been obtained by means of conventional tensile tests [23–25].

Once $J_{SP}$ has been determined, fracture mechanics relationships, such as eq. (2), can be applied to obtain the estimation of the material fracture toughness in stress intensity factor units, $K_J^{SP}$, at crack initiation (assuming small scale yielding) [4,26,28].

$$\boldsymbol{K_J^{SP}} = \sqrt{\frac{\boldsymbol{E\,J_{SP}}}{1-\nu^2}} \tag{2}$$

where $E$ represents the Young modulus of the material and $\nu$ is the Poisson's ratio.

## 4. Master curve approach

The Master Curve is a probabilistic approach that enables the direct estimation of fracture properties in the transition zone of ferritic steels [29]. According to this approach, the dependence of fracture toughness with temperature can be defined by a mathematical model and a single parameter: the reference temperature ($T_0$). It represents the temperature at which the median of the $K_{Jc}$ distribution from 1 T (25 mm thick) size specimens is equal to 100 MPa.m$^{0.5}$ and is the only material dependent parameter required [4].

In addition, this approach considers the (statistical) effects of the thickness of the specimens on the fracture toughness values, as well as the scatter of the results in the DBTR. This reduces significantly the number of tests needed to be performed.

As a result, $T_0$ can be obtained with reduced volumes of material and with relatively small samples [4]. This has turned the approach into an advantageous solution to characterise the DBTR of ferritic steels, evidenced by its incorporation into numerous codes and standards [1–4].

According to the Master Curve, the value of $K_{Jc}$ for a given thickness ($B$, in mm), $K_{Jc}[B]$, should be converted into the corresponding fracture toughness in a 1 T (25 mm thick) specimen, $K_{Jc}$[1T]. This is performed by using eq. (3) [4]:

$$\boldsymbol{K_{Jc}}\,[1\mathrm{T}] = 20 + [\boldsymbol{K_{Jc}}[\boldsymbol{B}] - 20]\cdot\left(\frac{\boldsymbol{B}}{25.4}\right)^{1/4} \tag{3}$$

For the case being analysed, considering that the thickness of SP specimens is 0.5 mm, this implies that the $K_{Jc}$ estimation from small punch tests corresponding to a 1 T specimen, $K_{Jc}^{SP}$ [1T], is obtained from the $K_{Jc}^{SP}$ estimated with eq. (2) corresponding to 0.5 mm-thickness, $K_{Jc}^{SP}$[0.5]:

$$\boldsymbol{K_{Jc}^{SP}}\,[1\mathrm{T}] = 20 + \left[\boldsymbol{K_{Jc}^{SP}}[0.5] - 20\right]\cdot\left(\frac{0.5}{25.4}\right)^{1/4} \tag{4}$$

## 5. Results and discussion

Small punch tests on specimens with a lateral notch of 4.4 mm have been performed at different temperatures, ranging from 158 to 93 K, for the estimation of the reference temperatures of the materials analysed. Figs. 7–10 show the Force-Displacement curves obtained from the tests. Six tests have been performed per material, according to the recommendations of [4]. From the discontinuity on the slope of the curves, it can be seen that in all cases a crack has initiated during the test, which was also confirmed by means of visual inspection of the specimen after the tests. A detail of a ruptured small punch specimen can be seen in Fig. 11.

To guarantee that the Master Curve approach can be applied, the

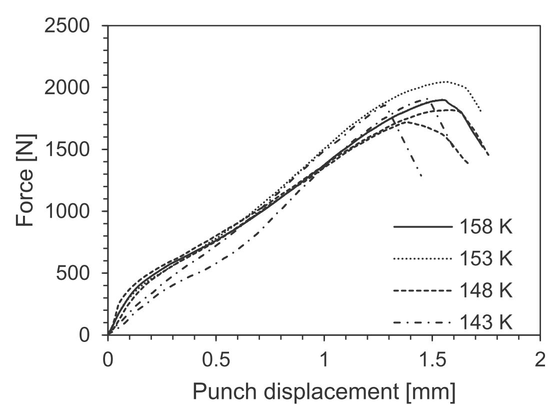


**Fig. 7.** Force-displacement curves obtained for A533B plate.

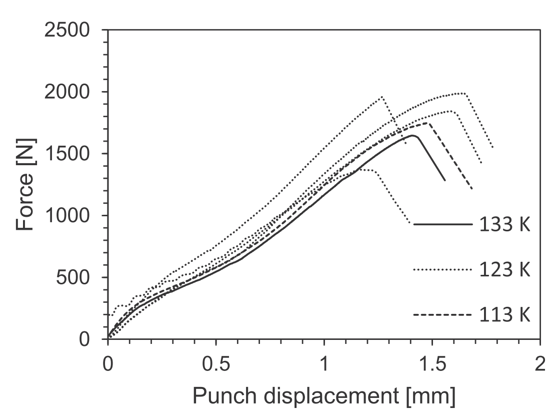


**Fig. 8.** Force-displacement curves obtained for S275JR.

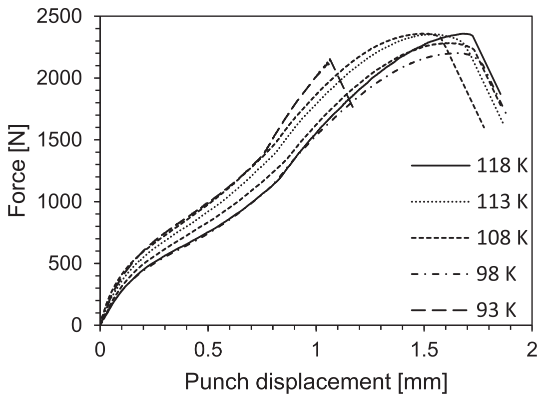


**Fig. 9.** Force-displacement curves obtained for S460M.

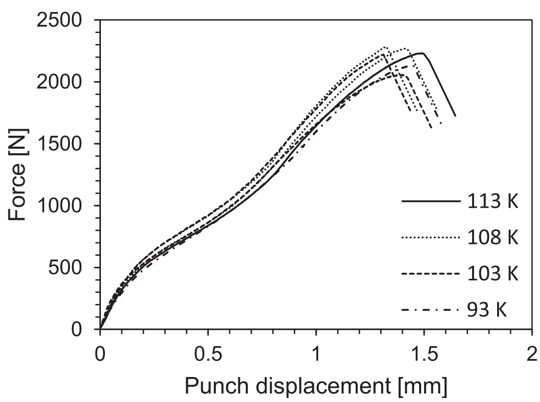


**Fig. 10.** Force-displacement curves obtained for S690Q.

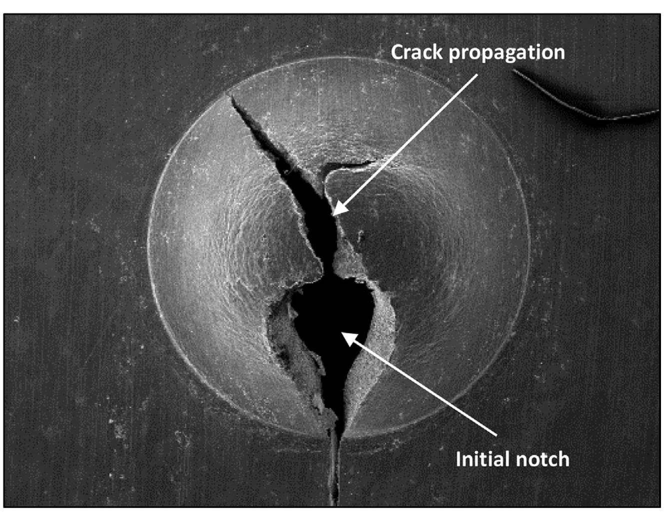


**Fig. 11.** Detail of a ruptured small punch specimen of S690Q. The deformation of the notch can be seen, which has led to the initiation of a crack.

onset of cleavage cracking has been a criterion for the acceptance of the tests as valid for the estimation of the reference temperature. On the Force-Displacement curves, it can be identified as a sudden drop of the load at maximum force or as a discontinuity in its proximity [5]. Stable cracking, exhibiting ductile mechanisms, can be expected in those curves not exhibiting such discontinuity.

The validity criterion of the small punch tests for the estimation of the reference temperature has been validated with the analysis of the fracture micro-mechanisms present at the crack initiation, as shown in Fig. 12. It can be seen that those specimens suffering a sudden load drop at maximum force exhibit a brittle fracture (Fig. 12 A), while those with a discontinuity on its slope exhibit a mixed mechanism of fracture, with cleavages present on it after some ductile tearing (Fig. 12 B). Finally, tests performed at room temperature which do not show such discontinuity exhibit a fully

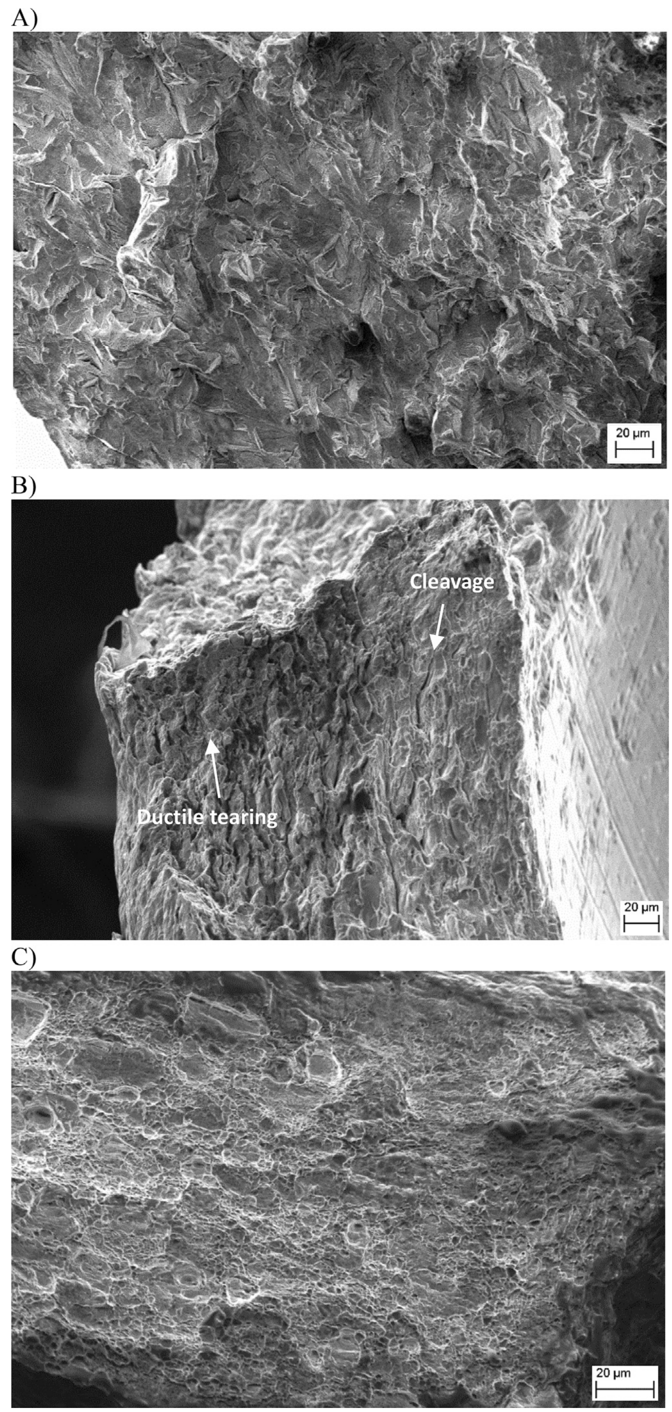


**Fig. 12.** A) Detail of a ruptured small punch specimen that experienced a sudden load drop at rupture, B) Detail of a ruptured small punch specimen that experienced a disconuity on the slope at maximum force, C) Detail of a ruptured small punch specimen at room temperature.

ductile fracture, as shown in Fig. 12 C.

Consequently, it is recommended to analyse the micro-mechanisms in case of doubt after the performance of the small punch tests, in order to guarantee the validity criterion proposed here and the correct approximation to the master curve approach. This further analysis is not necessary for tests exhibiting a sudden load drop at maximum force, where a brittle fracture is guaranteed.

From the tests performed, $K_{Jc}^{SP}$ [1T] values have been estimated following the aforementioned approach, the results being shown in Table 3. The tensile properties, which have been obtained at room temperature, have been transformed to their equivalent values at each temperature according to the recommendations of BS 7910 [2] before applying them to eqs. (1) and (2) or to $d_n$ [27].

The small punch reference temperature corresponding to each material has been determined according to the standard ASTM E-1921 [4]. In Figs. 13–16, the small punch Master Curves for 5, 50 and 95% failure probabilities have been represented. The estimations obtained from the small punch tests fit accurately within the predicted curves, confirming the suitability of the methodology. The obtained $T_0^{SP}$ values are shown on Table 4. It can be seen that the reference temperature obtained by means of small punch tests is lower than the values obtained by means of full scale conventional tests. Consequently, a relationship between both reference temperatures needs to be established. To achieve this goal, both values have been compared in Fig. 17.

As seen in Fig. 17, the reference temperature, in K, obtained by means of small punch tests is approximately half of the corresponding value obtained by means of full-scale conventional tests, with accurate results for the four materials analysed. The difference between $T_0$ and $T_0^{SP}$ might be not related to absolute specimen size, but to the influence of the specimen geometry and loading mode on the cleavage toughness, in a similar way to the differences between C(T) and SE(B) specimens or specimens with deep and shallow cracks [30].

The obtained coefficient is slightly different from the first value obtained in the first approach on materials SA-508M and S275JR [5], where instead of a 0.49 coefficient between $T_0^{SP}$ and $T_0$, a coefficient of 0.65 was obtained. The reason for this shift could be due to

**Table 3**
Results obtained from the small punch tests performed.

| MATERIAL | $T$ [K] | $\delta_{SP}$ [mm] | $d_n$ | $J_{SP}$ [kN/M] | $K_{Jc}^{SP}$ [1T] [MPa.m$^{0.5}$] |
|---|---|---|---|---|---|
| A533B | 158 | 0.58 | 0.87 | 429 | 133 |
| | 153 | 0.71 | 0.88 | 528 | 147 |
| | 148 | 0.64 | 0.89 | 480 | 140 |
| | 148 | 0.43 | 0.89 | 322 | 117 |
| | 143 | 0.37 | 0.90 | 280 | 110 |
| | 143 | 0.57 | 0.90 | 431 | 134 |
| S275JR | 133 | 0.53 | 0.83 | 356 | 123 |
| | 123 | 0.40 | 0.87 | 272 | 109 |
| | 123 | 0.35 | 0.87 | 238 | 103 |
| | 123 | 0.65 | 0.87 | 442 | 136 |
| | 123 | 0.63 | 0.87 | 429 | 134 |
| | 113 | 0.41 | 0.90 | 288 | 112 |
| S460M | 118 | 0.71 | 0.96 | 567 | 152 |
| | 113 | 0.86 | 0.97 | 698 | 168 |
| | 108 | 0.88 | 0.99 | 721 | 170 |
| | 108 | 0.70 | 0.99 | 573 | 153 |
| | 98 | 0.56 | 1.00 | 483 | 142 |
| | 93 | 0.19 | 1.00 | 170 | 89 |
| S690Q | 113 | 0.42 | 0.96 | 472 | 140 |
| | 108 | 0.30 | 0.97 | 341 | 121 |
| | 108 | 0.26 | 0.97 | 296 | 113 |
| | 103 | 0.52 | 0.98 | 598 | 156 |
| | 103 | 0.36 | 0.98 | 414 | 132 |
| | 93 | 0.54 | 0.99 | 647 | 162 |

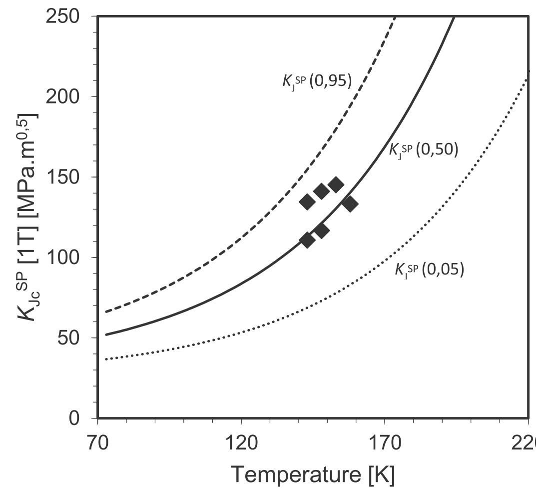


**Fig. 13.** Small punch master curves of A533B plate for 5, 50 and 95% failure probabilities.

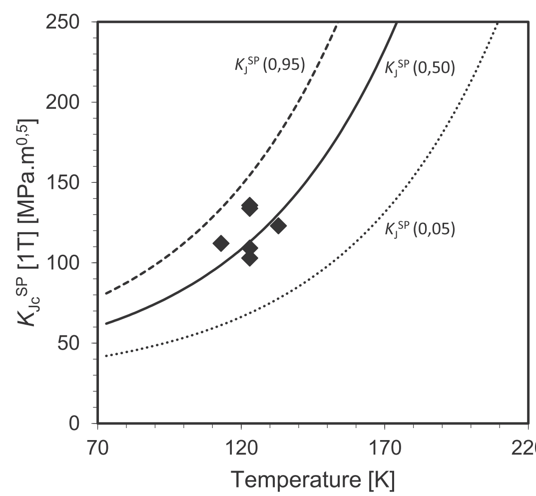


**Fig. 14.** Small punch master curves of S275JR plate for 5, 50 and 95% failure probabilities.

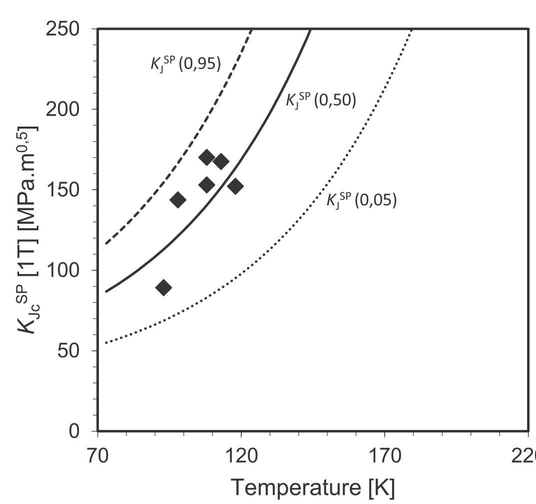


**Fig. 15.** Small punch master curves of S460M plate for 5, 50 and 95% failure probabilities.

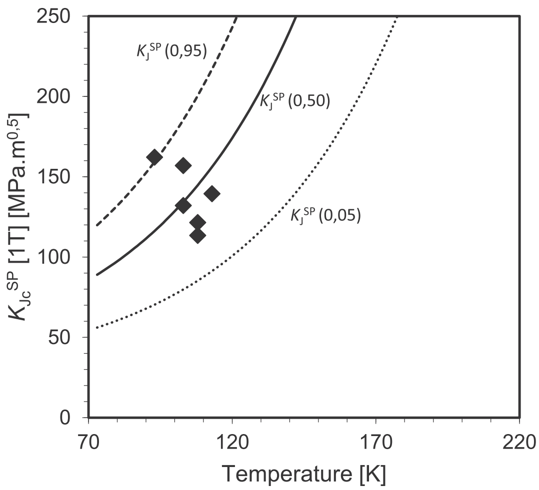


**Fig. 16.** Small punch master curves of S690Q plate for 5, 50 and 95% failure probabilities.

**Table 4**
Small punch reference temperature values obtained for each material.

| MATERIAL | A533B | S275JR | S460M | S690Q |
|---|---|---|---|---|
| $T_0^{SP}$ **[K]** | 134 | 114 | 84 | 82 |

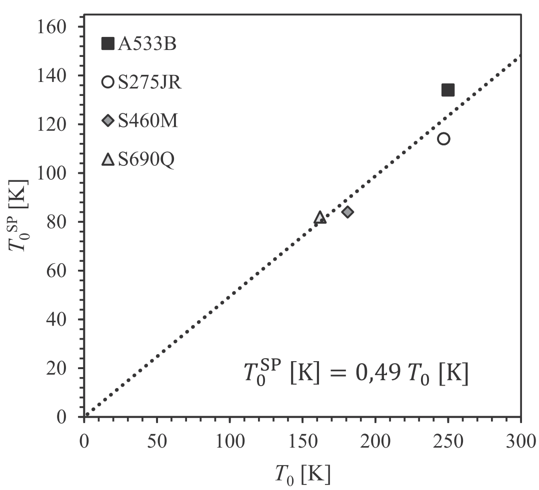


**Fig. 17.** Relationship between the reference temperature obtained by means of small punch tests and by means of full scale conventional testing techniques.

the use of different testing rigs. In this research, special care was given to guarantee that specimen geometry tested was the same in all cases. This was attained by means of the use of a newly designed adjustable lower matrix. In the aforementioned research [5], conventional testing rigs were used, which could have led to some clearance between the specimen and the rig, therefore modifying the tested notch length. Further analysis of the influence of the notch length should be performed in the future to gain further understanding of its possible effects.

## 6. Conclusions

Small punch modified specimens, with a lateral notch, in combination with the Master Curve approach have been applied successfully to characterise the ductile to brittle transition region of a pressure vessel steel and three different structural steels. A methodology has been proposed, including a validity criterion for the performed tests. In addition, a single correlation between the reference temperature obtained by means of full-scale conventional tests and small punch tests has been established.

Further testing should be performed on other materials, to confirm the accuracy of the proposed relationship. Special care should be paid to geometry of the specimen and to the correct alignment of the notch during the tests. The effects of the notch geometry should be analysed in order to better understand its influence.

In conclusion, this paper confirms the suitability of the small punch test for the characterisation of the DBTR of ferritic steels. The use of this testing technique in combination with the Master Curve approach allows the evaluation of the DBTR with highly reduced volumes of material. This feature is especially relevant when compared with other sub-size specimens, such as microCT's, since small punch specimens represent only 1/8th of the volume of a microCT specimen. Furthermore, it is a simple and cost-effective test, which can be performed with simple equipment.

## Data availability

The raw data required to reproduce these findings are available to download from https://www.opendataccfe.org/. The processed data required to reproduce these findings are available to download from https://www.opendataccfe.org/.

## Acknowledgements

This work was supported by the RCUK Energy Programme [grant number EP/P012450/1] and the Ministry of Economy, Industry and Competitiveness of the Spanish Government [grant number MAT2014-58738-C3-3-R]. To obtain further information on the data and models underlying this paper please contact PublicationsManager@ukaea.uk*.

## APPENDIX A

To gain further confidence on the lack of influence on the results of the use of 8 mm-diameter or 10 mm-square specimens, finite element simulations have been performed. Simulations of small punch tests on S460M steel at 173 K have been carried out on both geometries. An elastoplastic continuum mechanics finite element model realised via ANSYS, version 18.0 has been used. For the round specimen, a 2D axisymmetric model has been used, while for the square specimen a 3D model has been applied, simulating only 1/4th of the specimen given the symmetry, as shown in Fig. 18. The applied material properties have been derived from conventional testing, by using the elastic modulus of the material and a Ramberg-Osgood model for the hardening of the material, as shown in eq. (5). Frictional contacts have been employed, with a friction coefficient of 0.21.

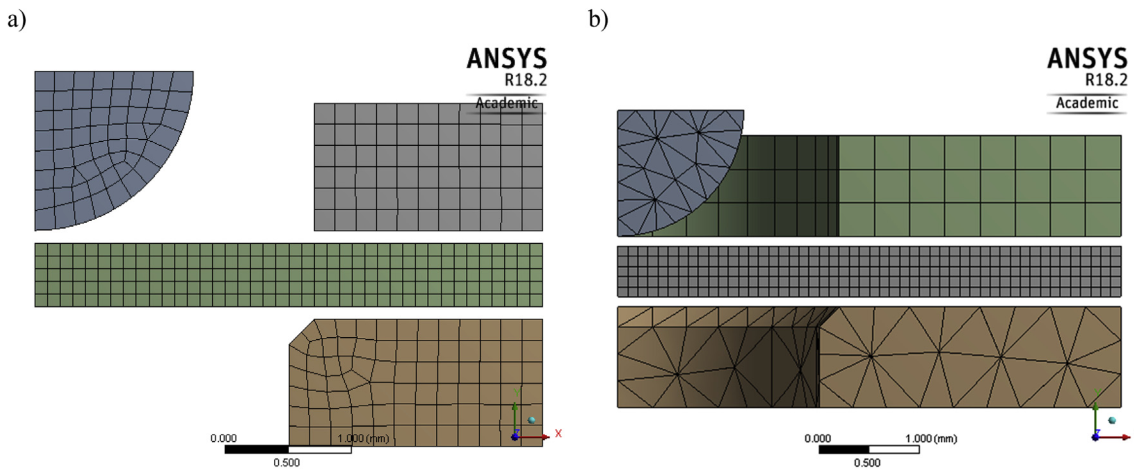


**Fig. 18.** A) 2D Model of a 8 mm-diameter round small punch specimen, B) 3D Model of a 10 mm-square small punch specimen.

$$\varepsilon = \frac{\sigma}{E} + K\left[\frac{\sigma}{E}\right]^{n} \quad (5)$$

In eq. (5), $\varepsilon$ is the strain, $\sigma$ is the applied stress, $E$ is the Young modulus (212,000 MPa) and $K$ and $n$ are the Ramberg-Osgood parameters, which have been estimated form conventional tensile tests (5.83e20 and 7.93, respectively).

The results obtained from the aforementioned simulations are shown in Fig. 19. As it can be seen, the two curves are coincident, showing a minor deviation closed to the maximum force, which might be probably influenced by the different size of the meshes of the dies and the punch. Consequently, no effect has been considered on the use of 10 mm-square specimens instead of the 8 mm-diameter round specimens, on agreement with the future small punch standard [8].

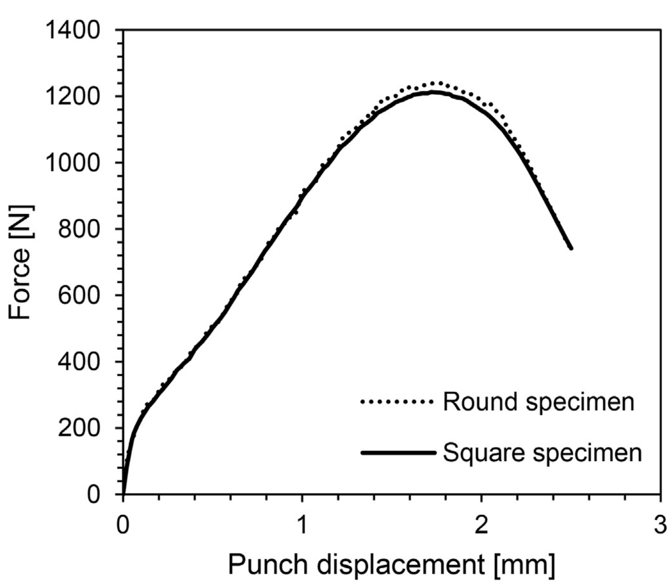


**Fig. 19.** Results obtained from the simulations with two different specimen geometries.

## References


[1] C. Berger, J.G. Blauel, L. Hodulak, B. Pyttel, I. Varfolomeyev, Fracture mechanics proof of strength for engineering components, in: Forschungskuratorium Maschinenbau (FKM), VDMA, Frankfurt a.M., 2009, 3rd rev.ed.

[2] B. Standard, BS 7910: 2013+ A1: 2015 Guide to Methods for Assessing the Acceptability of Flaws in Metallic Structures, BSI Stand. Ltd, 2013.

[3] A.S. Of Mechanical Engineers, API 579-1/ASME FFS-1 Fitness-For-Service, American Society of Mechanical Engineers, 2016.

[4] ASTM E1921-18a, Standard Test Method for Determination of Reference Temperature, to, for Ferritic Steels in the Transition Range, ASTM International, West Conshohocken, PA, 2018. www.astm.org.

[5] R. Lacalle, D. Andres, J.A. Alvarez, F. Gutierrez-Solana, Transition region of nuclear vessel steels: master curve approach using small punch notched specimens, in: Small Sample Test Tech., Trans Tech Publications, 2017, pp. 77–86, https://doi.org/10.4028/www.scientific.net/KEM.734.77.

[6] R. Chaouadi, E. van Walle, M. Scibetta, R. Gérard, On the Use of Miniaturized CT Specimens for Fracture Toughness Characterization of RPV Materials, 2016, https://doi.org/10.1115/PVP2016-63607. V01BT01A014.

[7] M. Yamamoto, A. Kimura, K. Onizawa, K. Yoshimoto, T. Ogawa, A. Chiba, T. Hirano, T. Sugihara, M. Sugiyama, N. Miura, N. Soneda, A Round Robin Program of Master Curve Evaluation Using Miniature C(T) Specimens: First Round Robin Test on Uniform Specimens of Reactor Pressure Vessel Material, 2012, pp. 73–79. https://doi.org/10.1115/PVP2012-78661.

[8] M. Bruchhausen, T. Austin, S. Holmström, E. Altstadt, P. Dymacek, S. Jeffs, R. Lancaster, R. Lacalle, K. Matocha, J. Petzová, European Standard on Small Punch Testing of Metallic Materials, 2017. V01AT01A065, https://doi.org/10.1115/PVP2017-65396.

[9] R. Lacalle, J.A. Álvarez, B. Arroyo, F. Gutiérrez-Solana, Methodology for fracture toughness estimation based on the use of Small Punch notched specimens and the CTOD concept, in: Proc. 2nd Int. Conf. SSTT, 2012.

[10] R. Lacalle, J.A. Álvarez, F. Gutiérrez-Solana, Use of small punch notched specimens in the determination of fracture toughness, in: ASME 2008 Press. Vessel. Pip. Conf., vol. 6, 2008, pp. 1363–1369.

[11] M.P. Manahan, A.S. Argon, O.K. Harling, The development of a miniaturized disk bend test for the determination of postirradiation mechanical properties, J. Nucl. Mater. 104 (1981) 1545–1550, https://doi.org/10.1016/0022-3115(82)90820-0.

[12] C.W.A. 15627 CEN Workshop Agreement, Small Punch Test Method for Metallic Materials, 2007.

[13] T. Linse, M. Kuna, H.W. Viehrig, Quantification of brittle-ductile failure behavior of ferritic reactor pressure vessel steels using the Small-Punch-Test and micromechanical damage models, Mater. Sci. Eng. A 614 (2014) 136–147, https://doi.org/10.1016/j.msea.2014.05.095.

[14] R. Lacalle, Determinación de las propiedades de tracción y fractura de materiales metálicos mediante ensayos small punch (Doctoral Thesis), Univ. Cantab., 2012.

[15] X. Mao, H. Takahashi, Development of a further-miniaturized specimen of 3 mm diameter for tem disk (ø 3 mm) small punch tests, J. Nucl. Mater. 150 (1987) 42–52, https://doi.org/10.1016/0022-3115(87)90092-4.

[16] M. Abendroth, M. Kuna, Identification of ductile damage and fracture parameters from the small punch test using neural networks, Eng. Fract. Mech. 73 (2006) 710–725.

[17] J.B. Ju, J.I. Jang, D. Kwon, Evaluation of fracture toughness by small-punch testing techniques using sharp notched specimens, Int. J. Press. Vessel. Pip. 80 (2003) 221–228.

[18] E. Martínez-Pañeda, T.E. García, C. Rodríguez, Fracture toughness characterization through notched small punch test specimens, Mater. Sci. Eng. A 657 (2016) 422–430, https://doi.org/10.1016/j.msea.2016.01.077.
[19] K. Turba, B. Gülcimen, Y.Z. Li, D. Blagoeva, P. Hähner, R.C. Hurst, Introduction of a new notched specimen geometry to determine fracture properties by small punch testing, Eng. Fract. Mech. 78 (2011) 2826–2833.
[20] D. Andrés, Caracterización mecánica mediante ensayos small punch de materiales metálicos sometidos a altas temperaturas (Doctoral Thesis), Universidad de Cantabria, 2017.
[21] E.UNE, m286-1, Especificación Geométrica Prod. (GPS)–Sistema ISO Para Las Toler. Dimens. Parte 1 Base Toler. Desviaciones Y Ajustes, 2010.
[22] D. Andrés, R. Lacalle, A. Jaurrieta, J.A. Álvarez, Optimización de la geometría de la entalla lateral pasante en la estimación de la tenacidad a fractura mediante probetas small punch, GEF 2018, Malaga, 2018.
[23] S. Cicero, T. Garcia, V. Madrazo, Application and validation of the notch master curve in medium and high strength structural steels, J. Mech. Sci. Technol. 29 (2015) 4129–4142, https://doi.org/10.1007/s12206-015-0907-2.
[24] M.A. Sokolov, D.E. McCabe, R.K. Nanstad, Y.A. Davidov, Use of Precracked Charpy and Smaller Specimens to Establish the Master Curve, 1997.
[25] T. García, S. Cicero, Application of the Master Curve to ferritic steels in notched conditions, Eng. Fail. Anal. 58 (2015) 149–164. Part 1.
[26] T.L. Anderson, T.L. Anderson, Fracture Mechanics: Fundamentals and Applications, third ed., Taylor \& Francis, 2005.
[27] C.F. Shih, Relationships between the J-integral and the crack opening displacement for stationary and extending cracks, J. Mech. Phys. Solids 29 (1981) 305–326, https://doi.org/10.1016/0022-5096(81)90003-X.
[28] ASTM Standard E-1820-15a, Standard Test Method for Measurement of Fracture Toughness, ASTM Int., 2011, https://doi.org/10.1520/E1820-11E01.
[29] K. Wallin, V.Teknillinen Tutkimuskeskus, E.C.P., Fracture T. Of steel in the ductile to brittle tension regime, in: Measurements, T. Programme, Master Curve Analysis of Ductile to Brittle Transition Region Fracture Toughness Round Robin Data: the “EURO” Fracture Toughness Curve, Technical Research Centre of Finland, 1998.
[30] J.A. Joyce, R.L. Tregoning, Quantification of specimen geometry effects on the master curve and to reference temperature, in: 13th Eur. Conf. Fract. San Sebast, 2000.